Kobayashi, H., Komatsu, K., Ito, H., Machida, S., Hattori, T., & Kagi, H. (2023). Slightly hydrogen-ordered state of ice IV evidenced by in situ neutron diffraction. *The Journal of Physical Chemistry Letters*, *14*(47), 10664-10669. DOI: 10.1021/acs.jpclett.3c02563

Slightly Hydrogen-Ordered State of Ice IV Evidenced by *In-Situ* Neutron Diffraction

Hiroki Kobayashi[1], Kazuki Komatsu[1], Hayate Ito[1], Shinichi Machida[2], Takanori Hattori[3], and Hiroyuki Kagi[1]*

[1] Geochemical Research Center, Graduate School of Science, The University of Tokyo, 7-3-1, Hongo, Bunkyo-ku, Tokyo, 113-0033, Japan

[2] Neutron Science and Technology Center, Comprehensive Research Organization for Science and Society (CROSS), 162-1 Shirakata, Tokai, Naka, Ibaraki, 319-1106, Japan

[3] J-PARC Center, Japan Atomic Energy Agency. 2-4 Shirakata, Tokai, Naka, Ibaraki, 319-1195, Japan

Corresponding author.

*E-mail: hiroki@eqchem.s.u-tokyo.ac.jp

ABSTRACT. Ice IV is a metastable high-pressure phase of ice in which the water molecules exhibit orientational disorder. Although orientational ordering is commonly observed for other ice phases, it has not been reported for ice IV. We conducted *in-situ* powder neutron diffraction experiments for DCl-doped D_2O ice IV to investigate its hydrogen ordering. We found abrupt changes in the temperature derivative of unit-cell volume, dV/dT, at ~120 K, and revealed a slightly ordered structure at low temperatures based on the Rietveld method. The occupancy of the D1 site deviates from 0.5 in particular; it increased when samples were cooled at higher pressures and reached 0.174(14) at 2.38 GPa, 58 K. Our results evidence the presence of a low-symmetry hydrogen-ordered state corresponding to ice IV. It seems, however, difficult to experimentally access the completely ordered phase corresponding to ice IV by slow cooling at high pressure.

TOC Graphics

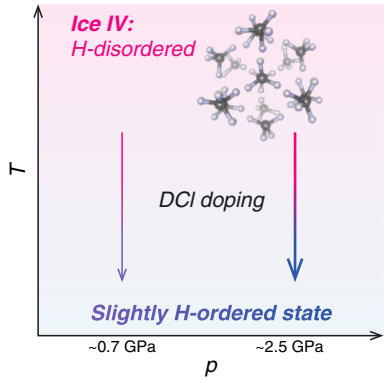

Keywords: ice IV, high pressure, polymorphs, powder neutron diffraction, orientational order

Water is a ubiquitous material being studied in a wide range of research fields. Water molecules form tetrahedral networks in hydrogen-bonded structures while maintaining freedom in the orientation of the dipole moment. Hence, states with molecular orientational order and disorder are both possible in a given oxygen sublattice in ice. Such hydrogen-ordered and disordered phases can be distinguished based on hydrogen-site occupancies in time-space averaged structures determined by diffraction experiments. Disordered phases are thermodynamically stable in high-temperature regions. As the temperature decreases, hydrogen-ordered structures become more stable, driving hydrogen disorder-to-order phase transitions without changing the oxygen sublattice. This makes the polymorphism of ice very rich. The search for new ordered phases corresponding to known disordered ones is one of the most successful strategies of new-phase discoveries in recent years.[1–5] However, experimental access to ordered phases is kinetically challenging because molecular reorientation dynamics slows with decreasing temperatures and finally freezes at the orientational glass transition temperature (often referred to as T_g). To enhance molecular reorientation and suppress orientational glass formation, it is effective to dope disordered phases with a small amount of acid or base. It is known that KOH doping effectively promotes the ice I_h-to-XI disorder-to-order transformation[6,7] and HCl doping does the ice V-to-XIII,[1,8,9] VI-to-XV,[2,8,10,11] and XII-to-XIV[1,12–14] transitions.

In this study, we focus on a metastable high-pressure phase ice IV.[15] Except for superionic ice XVIII,[16] ice IV is the only high-pressure hydrogen-disordered phase whose ordered counterpart has not been reported to date. It is interesting to investigate the hydrogen-ordering behavior of ice IV not

57 only because it may lead to the discovery of a new phase but also because the hydrogen-disordered
58 structures of ices I and IV have been suggested to be related to the pressure-induced amorphization
59 mechanism of ice I_h into high-density amorphous ice (HDA); it was suggested that the local structure
60 of HDA is similar to the structure of ice IV[17,18] and HDA is a "derailed" state of the ice I-IV
61 transformation pathway due to hydrogen disorder in these crystalline phases.[17] Quests for a hydrogen-
62 ordered counterpart of ice IV have been made based on *ex-situ* experiments using Raman
63 spectroscopy,[19] differential scanning calorimetry (DSC),[20,21] and powder X-ray diffraction[21]
64 techniques by Salzmann and co-workers. They prepared ice IV samples by heating HDA, quenched
65 the samples to liquid nitrogen temperature, and released the pressure to recover them for analyses at
66 ambient pressure. According to their *ex-situ* DSC investigations, HCl-doped ice IV showed a weak
67 irreversible endothermic feature at ~120 K upon heating at ambient pressure whereas nondoped and
68 LiOH-doped samples did not. Furthermore, the endotherms were more pronounced when samples were
69 annealed at higher pressures. These results suggest that there is a low-temperature state related to ice
70 IV that (i) can be obtained only when HCl is doped, (ii) is more favored at higher pressures, and (iii)
71 is not obtained by cooling doped ice IV at ambient pressure. The origin of the endotherms remains
72 unclear as Rosu-Finsen and Salzmann (2021) listed three possible causes to explain the results:
73 hydrogen ordering, orientational glass transition, and release of strain.[21] To better understand the
74 pressure-temperature response of doped ice IV and to corroborate a novel ordered phase if it exists, *in-*
75 *situ* experiments with high sensitivity to hydrogen ordering are desired.

In this study, we conducted *in-situ* powder neutron diffraction experiments at the high-pressure neutron diffractometer *PLANET*[22] in the Materials and Life Science Experimental Facility (MLF) of J-PARC using a temperature-variable hydraulic press *Mito system*.[23] See Supporting Information for detailed methods. Ice IV doped with DCl was prepared from HDA.[24] After the crystallization of ice IV was completed, the sample was slowly cooled while powder neutron diffractograms were collected continuously. We present the results of three experiments in this article (Exps. #1–3); please refer to Figure S1 for the pressure–temperature histories in each experiment.

The unit-cell volume and the lattice parameters of DCl-doped D_2O ice IV as functions of temperature (Exp. #1) are shown in Figure 1a,b. Upon lowering the temperature, the slope of the temperature dependence of the unit-cell volume abruptly changed at around 120 K, suggesting a structural transition to a low-temperature state (Figure 1a, blue plots). Unfortunately, perfect isobaric cooling is impossible with our high-pressure instrumentation using an opposed-anvil-type apparatus as indicated by the purple curve in Figure 1a. Because these unavoidable pressure changes should contribute to the lattice expansion, one may question whether the dV/dT change was a result of the structural change of the sample or merely originated from the changes in the sample pressure. To clarify this, we use the isothermal compressibility of disordered ice IV by using a data set collected at 157 K (pressure range: from 0.59(1) GPa to 2.53(1) GPa). The lattice parameters a and c as well as unit-cell volume V decreased linearly upon increasing pressure at 157 K (Figure S2). However, in Exp. #1, the a-axis (in the hexagonal setting) showed an abrupt change while the c-axis length showed a monotonic decrease

with decreasing temperature (Figure 1b). There also seems to be a bent in c/a as indicated by a dotted arrow in Figure 1b. It is unlikely that there is an unusual pressure response that appears only on the a-axis while both the a- and c-axis lengths change linearly with pressure in ice IV. The results of Exp. #2 (Figure 1c,d), in which DCl-doped D_2O ice IV was cooled at slightly higher pressures, also support that the anomalous changes in dV/dT were temperature-induced phenomena.

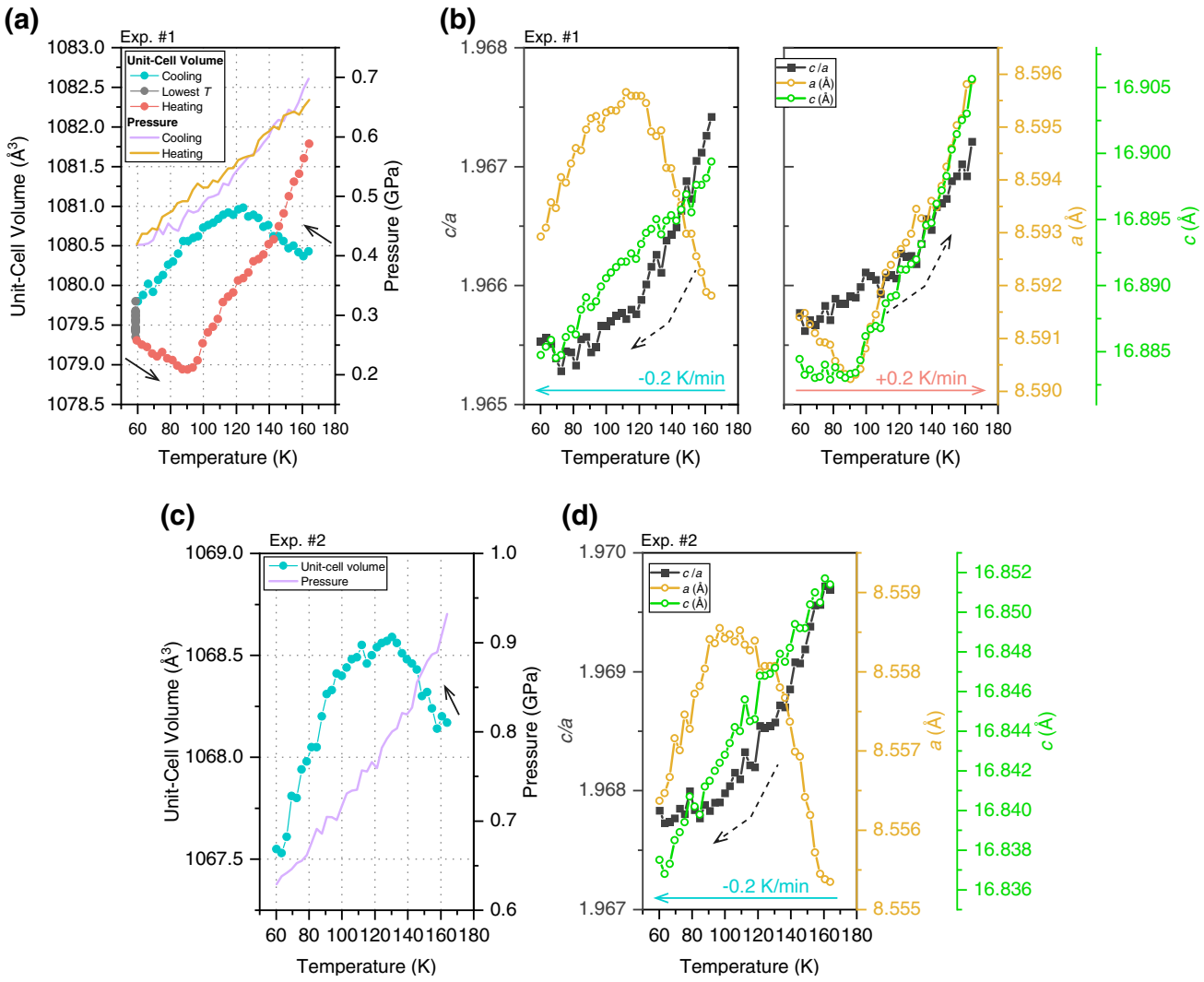

Figure 1. Temperature dependence of the unit-cell volume and lattice parameters (Exps. #1 and #2). Experiment ID is shown in each panel. **(a, c)** Unit-cell volume and pressure determined from the Pb pressure marker as functions of temperature. **(b, d)** Lattice parameters *a* and *c*, and their ratio *c*/*a*.

In Exp. #1, the DCl-doped ice IV sample was thereafter kept at 58 K and 0.42 GPa for 6 h. The neutron diffraction pattern collected at 58 K was time-sliced by 15 min to track changes in the lattice parameters (Figure 1a, gray plots). Interestingly, the unit-cell volume slightly and continuously decreased with time. Since the sample pressure estimated from the lead pressure marker was constant in these measurements at 58 K, this continuous lattice contraction is probably caused by the progress of the structural conversion from ice IV to the low-temperature state. After 6 h, the sample was heated up to 165 K at 0.2 K/min. In Figure 1(a), unit-cell volume seems irreversible to temperature. First, the onset temperatures of the dV/dT changes are ~120 K and ~90 K in cooling and heating, respectively. The temperature relation is opposite to the hysteresis observed in normal first-order phase transitions. Moreover, the temperatures of the dV/dT (or da/dT) and d(c/a)/dT changes seem not to be matched in the heating pathway. Unfortunately, the origin of these complicated kinetic features in the backward transformation pathways involving the inverted hysteresis remains unclear at present. Second, the T–V plot in Figure 1a is not a closed loop, as the unit-cell volumes at the starting and ending points differ. However, these disagreements in unit-cell volume can be again attributed to pressure variation during heating. The observed difference in the unit-cell volume at the starting and ending points in Figure 1a

(ΔV = 1.4(5) Å^3) agreed well with the volume difference (ΔV = 1.5(6) Å^3) estimated from the pressure difference (Δp = 0.035(10) GPa) at these points using the linear fitting of the compressibility data (Figure S2). Thus, we suggest that the sample returned to the original structure (*i.e.,* as-crystallized ice IV) after cooling and heating.

Because the volume changes were very small, we should rely on more direct structural information to firmly discuss the presence and nature of the low-temperature state. The diffraction profiles collected in our experiments showed no additional Bragg-reflection emergence compared to as-crystallized ice IV, and therefore diffraction patterns were analyzed using the original space group of ice IV ($R\bar{3}c$[25]), or its only subgroup having the same reflection conditions ($R3c$). The number of crystallographic sites is doubled due to the loss of mirror symmetry from $R\bar{3}c$ to $R3c$ (Tables S1 and S2). In $R\bar{3}c$, only deuterium atoms at two sites (D4 and D5) out of six are permitted to order while all deuterium atoms can at least partially order in $R3c$. We tested both space-group candidates in Rietveld analyses to the diffractogram of DCl-doped D_2O ice IV collected at 58 K, 0.42 GPa (Exp. #1), allowing all possible deuterium sites to order. The χ^2 value was improved from 8.445 to 7.473 by applying the low-symmetry space group $R3c$ (Figure S3). We found some peaks fitted better in $R3c$ (Figure S3) although the difference of χ^2 is small between the two. In the $R\bar{3}c$ model, the refined occupancies of the D4 and D5 sites are 0.505(1) and 0.495(1), respectively, which indicate nearly perfect hydrogen disorder. By contrast, the $R3c$ model is slightly hydrogen ordered in which the ordering parameter o_1, which equals the occupancy of the D1 site, was 0.356(5) (Table S1). Here, please note that the

occupancy of this D1 site is fixed at 0.5 in $R\bar{3}c$ and is a variable only in $R3c$. A slightly ordered structure was also obtained from the data collected at 58 K, 0.63 GPa in Exp. #2 (Table S3). To crosscheck the reliability of the results, data collected at 165 K after the cooling-heating experiments (Exp. #1) was also Rietveld-analysed using both $R\bar{3}c$ and $R3c$ space groups. Even when refined using the $R3c$ space group, the structure at 165 K was suggested to be disordered within estimated errors where the ordering parameters o_1, o_2, and o_3 were 0.53(5), 0.506(3), and 0.506(3), respectively; *i.e.,* the most plausible space group for the structure at 165 K is $R\bar{3}c$ (see Table S2 for the refined structure parameters assuming perfect disorder). This suggests that the order-to-disorder transformation was completed during heating. These results suggest that (i) when slowly cooled, hydrogen ordering in DCl-doped ice IV proceeds at temperatures below ~120 K, but (ii) the hydrogen-ordering transition is hampered due to slow transformation kinetics at low temperatures.

To investigate the effects of pressure on hydrogen ordering, we conducted another experiment (Exp. #3) in which DCl-doped D_2O ice IV was cooled from 157 K to 58 K at higher pressures from 2.64 to 2.37 GPa. At 157 K, the hydrogen-disordered structure of ice IV was maintained (refined ordering parameters using the $R3c$ space group: o_1 = 0.505(13), o_2 = 0.500(4), and o_3 = 0.499(3)); *i.e.,* there were no signs of a pressure-induced hydrogen ordering at this temperature. By contrast, Rietveld analysis to a diffractogram collected at 58 K converged into a partially ordered structure with the highest degree of ordering obtained in this study, although it is still small. An $R3c$ model better fits the diffractogram than an $R\bar{3}c$ model (Figure 2) as indicated by the improvement of χ^2 (χ^2 = 11.48 for

$R\bar{3}c$ and $\chi^2 = 10.51$ for $R3c$). The refined ordering parameters using the $R3c$ space group were $o_1 = 0.174(14)$, $o_2 = 0.554(10)$, and $o_3 = 0.486(8)$ which indicate orientational ordering during cooling, see Table 1 for the list of structure parameters. D1 and D1', which show relatively large degrees of hydrogen ordering, are located on the hydrogen bond penetrating the six-membered ring structure (Figure 2c). In Exp. #3, o_1 showed the largest deviation from 0.5 at 58 K among Exps. #1-3 (Figure 3), which is consistent with the previous *ex-situ* DSC studies suggesting that the low-temperature state is more favored at high pressures;[21] our neutron diffraction results also suggest the hydrogen ordering in ice IV is more pronounced at high pressures.

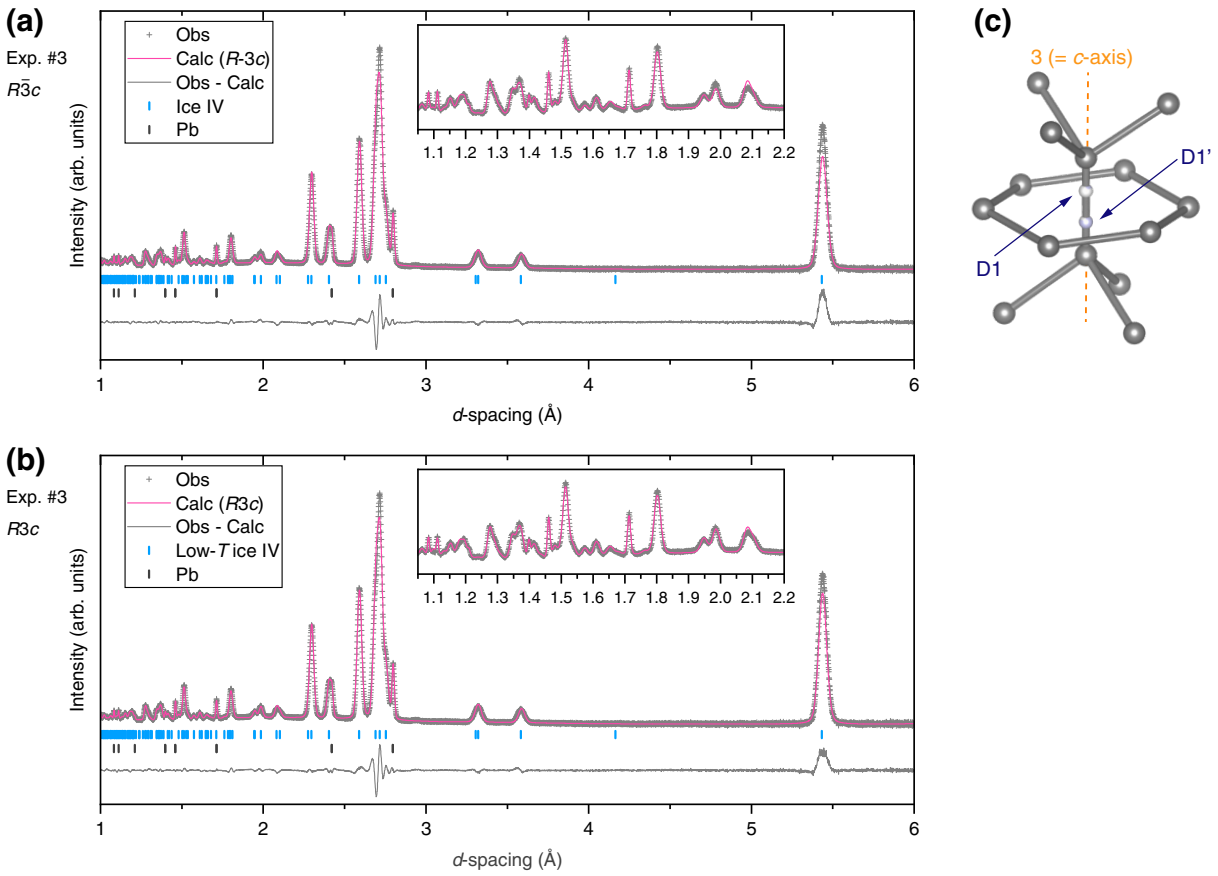

Figure 2. Structure analyses of the low-temperature state in the DCl-doped sample at 58 K, 2.38 GPa (Exp. #3). (a) Rietveld refinement using the $R\bar{3}c$ space group. χ^2 = 11.48, R_{wp} = 4.66%, R_p = 5.17%. The refined occupancies of deuterium sites were 0.5 within errors. **(b)** Rietveld refinement using the $R3c$ space group. χ^2 = 10.51, R_{wp} = 4.44%, R_p = 4.81%. **(c)** Building block of the structure of the low-temperature state. Gray balls represent oxygen atoms. Only deuterium atoms at the D1 and D1' sites, which showed the largest degree of ordering in the low-temperature state, are shown by white balls.

Table 1. Structure Model for the Low-Temperature State at 58 K, 2.38 GPa (Exp. #3) in the *R*3*c* Space Group.

Atom	*x*	*y*	*z*	Occupancy		U_{iso}
				Representation	Value	
O1	0.3729(9)	0.2539(14)	-0.0421(4)	1	1	0.0140(5)
O1'	0.6266(9)	0.7496(14)	0.94267(4)	1	1	0.0140(5)
O2	0	0	0.0366(8)	1	1	0.0140(5)
O2'	0	0	0.8702(7)	1	1	0.0140(5)
D1	0	0	-0.0198(9)	o_1	0.174(14)	0.0167(7)
D1'	0	0	0.9267(7)	$1 - o_1$	0.826(14)	0.0167(7)
D2	0.0137(6)	0.1146(5)	0.0501(7)	$\frac{2}{3} - \frac{1}{3}o_1$	0.609(5)	0.0167(7)

D2’	0.9590(7)	0.8914(7)	0.8403(7)	$\frac{1}{3}+\frac{1}{3}o_1$	0.391(5)	0.0167(7)
D3	0.4675(15)	0.2900(19)	0.9175(9)	$\frac{1}{3}+\frac{1}{3}o_1$	0.391(5)	0.0167(7)
D3’	0.5146(10)	0.7170(12)	-0.0266(7)	$\frac{2}{3}-\frac{1}{3}o_1$	0.609(5)	0.0167(7)
D4	0.3002(12)	0.3104(12)	0.9419(8)	o_2	0.554(11)	0.0167(7)
D4’	0.7294(14)	0.7282(15)	-0.0519(10)	o_3	0.486(8)	0.0167(7)
D5	0.3414(15)	0.1253(15)	-0.0350(9)	$1-o_2$	0.446(11)	0.0167(7)
D5’	0.6982(16)	0.8853(13)	0.9379(11)	$1-o_3$	0.514(8)	0.0167(7)
D6	0.3999(15)	0.2994(20)	0.0111(6)	$\frac{2}{3}-\frac{1}{3}o_1-o_2+o_3$	0.54(2)	0.0167(7)
D6’	0.5927(20)	0.699(2)	0.8909(5)	$\frac{1}{3}+\frac{1}{3}o_1+o_2-o_3$	0.46(2)	0.0167(7)

x, *y*, *z*: fractional atomic coordinates, U_{iso}: isotropic atomic displacement parameter. Deuterium-site occupancies are represented by three ordering parameters o_1, o_2, and o_3 to follow the ice rule (shown on the left in the column) with refined values shown on the right. $a = b = 8.32866(12)$ Å, $c = 16.5178(4)$ Å, $V = 992.28(3)$ Å^3.

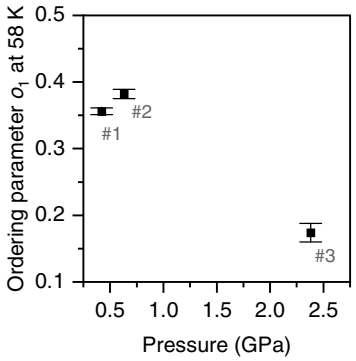

Figure 3. Values of the ordering parameter o_1 at 58 K refined from neutron diffraction patterns collected in Exps. #1-3. The space-group symmetry used in Rietveld analyses is $R3c$.

However, the overall degrees of hydrogen ordering remain low in the samples prepared in this study. In addition, $R3c$ cannot be the space group of a completely hydrogen-ordered ground-state phase corresponding to ice IV because occupancies of D2, D2', D3, D3', D6, and D6' sites are restricted to values between 1/3 and 2/3. There are several potential methods to increase the degree of orientational ordering in ice IV in future experiments. First, slower cooling or longer storage at low temperatures may allow doped ice IV samples to follow thermodynamic equilibrium more by reducing the kinetic effects and to achieve more ordered states. Second, our instrumentations with the *Mito system* are not capable of cooling liquid samples rapidly or precooling the sample chamber. As suggested in a previous study,[11,26] ice I_h obtained by slow cooling of liquid may result in insufficient DCl doping due to, for example, consumption of DCl by corrosion with metal gaskets or expelling of the DCl from crystalline ice. Such effects should be better understood to prepare more hydrogen-ordered samples. Third, dopants other than hydrochloric acid may be selectively effective for enhancing hydrogen ordering in ice IV. Fourth, novel methods, *e.g.*, fast cooling methods recently proposed in the ice XII-XIV disorder-order transition,[27] should be also tested.

To conclude, we investigated hydrogen ordering in ice IV employing *in-situ* neutron diffraction and reported crystallographic evidence of a slightly hydrogen-ordered state corresponding to ice IV for the

first time. DCl-doped deuterated ice IV showed abrupt changes in dV/dT and d(c/a)/dT at ~120 K. It is likely that the structural changes proceed very slowly at the temperatures below. The reverse hydrogen-disordering transformations during heating involve rather complicated features, which have not been perfectly interpreted yet. Rietveld analysis revealed hydrogen-disordered and slightly hydrogen-ordered structures above and below 120 K, respectively. $R3c$ is the best space group to describe the structure of the low-temperature state. The ordered state has a higher density than ice IV, making the structural conversion favorable at higher pressures as evidenced by experiments performed at ~2.5 GPa (Exp. #3). Among the three ordering parameters required to express deuterium-site occupancies in $R3c$, o_1, which equals the occupancy of the D1 site, showed the largest differences from the original value of 0.5 in the hydrogen-disordered ice IV. As with ices V, VI, and XII, acid doping effectively enhances hydrogen ordering in ice IV. However, even when DCl is doped, hydrogen ordering proceeds very slowly and the degrees of hydrogen ordering in the low-temperature state were small. The fully hydrogen-ordered counterpart of ice IV seems to have even more will-o'-the-wisp nature than the parent phase. Our results prompt inquiries into the thermodynamic and kinetic complexities behind hydrogen ordering in ice IV in comparison to other neighboring ice phases in which the ordered phase is accessible at pressures and temperatures comparable to those of our experiment.

Methods

Powder neutron diffraction experiments were conducted at the high-pressure neutron diffractometer *PLANET*[22] in J-PARC with the use of a temperature-variable hydraulic press *Mito system*.[23] A 4K GM refrigerator was installed instead of the use of liquid nitrogen cryogen, allowing us to cool samples down to 58 K, see a review paper by Komatsu (2022) for detailed specifications.[28] A piece of lead wire was loaded with the sample to estimate the sample pressure and the pressure was calculated based on the equation of state.[29] Collected neutron diffraction patterns were reduced and the observed intensities were corrected using in-house software at *PLANET*. Diffractograms were analyzed by the Rietveld method using the *GSAS* program on the *EXPGUI* package.[30,31] The *VESTA* software[32] was used to construct structure models in the $R3c$ space group and to visualize structures. Please refer to the Supporting Information for more details.

Ice IV was prepared following the established protocol by Salzmann *et al.,*[24] which involves cooling liquid water at 0 GPa to crystallize ice I_h, subsequent compression of ice I_h at 130-135 K for pressure-induced amorphization to yield HDA, and its heating at ~0.85 GPa at a rate of ~0.3 K/min. During heating HDA, sample pressure was monitored using Bragg peaks of lead, and the hydraulic pressure was manually controlled to achieve quasi-isobaric heating.

ASSOCIATED CONTENT

The Supporting Information is available free of charge at https://pubs.acs.org/doi/10.1021/acs.jpclett.3c02563?goto=supporting-info.

Detailed methods, pressure–temperature histories of each experiment, and crystallographic data (PDF)

AUTHOR INFORMATION

Notes

The authors declare no competing financial interest.

ACKNOWLEDGMENTS

Neutron diffraction experiments were conducted under J-PARC MLF user programs (Proposal Nos.: 2021B0159, 2022A0030, 2022B0093, 2023A0195). We are grateful to all the staff in J-PARC for supporting our experiments. H.Kobayashi and H.I. respectively thank the MERIT-WINGS and IGPEES programs of the University of Tokyo for support. This work is financially supported by JSPS Grants-in-Aid for Scientific Research "*KAKENHI"* (Grant Nos.: 18H05224, 21K18154).

REFERENCES

(1) Salzmann, C. G.; Radaelli, P. G.; Hallbrucker, A.; Mayer, E.; Finney, J. L. The Preparation and Structures of Hydrogen Ordered Phases of Ice. *Science.* **2006**, *311* (5768), 1758–1761. https://doi.org/10.1126/science.1123896.

(2) Salzmann, C. G.; Radaelli, P. G.; Mayer, E.; Finney, J. L. Ice XV: A New Thermodynamically Stable Phase of Ice. *Phys. Rev. Lett.* **2009**, *103* (10), 1–4. https://doi.org/10.1103/PhysRevLett.103.105701.

(3) Gasser, T. M.; Thoeny, A. V.; Plaga, L. J.; Köster, K. W.; Etter, M.; Böhmer, R.; Loerting, T. Experiments Indicating a Second Hydrogen Ordered Phase of Ice VI. *Chem. Sci.* **2018**, *9* (18), 4224–4234. https://doi.org/10.1039/C8SC00135A.

(4) Gasser, T. M.; Thoeny, A. V.; Fortes, A. D.; Loerting, T. Structural Characterization of Ice XIX as the Second Polymorph Related to Ice VI. *Nat. Commun.* **2021**, *12* (1). https://doi.org/10.1038/s41467-021-21161-z.

(5) Yamane, R.; Komatsu, K.; Gouchi, J.; Uwatoko, Y.; Machida, S.; Hattori, T.; Ito, H.; Kagi, H. Experimental Evidence for the Existence of a Second Partially-Ordered Phase of Ice VI. *Nat. Commun.* **2021**, *12* (1). https://doi.org/10.1038/s41467-021-21351-9.

(6) Tajima, Y.; Matsuo, T.; Suga, H. Phase Transition in KOH-Doped Hexagonal Ice. *Nature* **1982**, *299* (28), 810–812.

(7) Kawada, S.; Dohata, H. Dielectric Properties on 72 K Phase Transition of KOH-Doped Ice. *J. Phys. Soc. Japan* **1985**, *54* (2), 477–479. https://doi.org/10.1143/JPSJ.54.477.

(8) Rosu-Finsen, A.; Salzmann, C. G. Benchmarking Acid and Base Dopants with Respect to Enabling the Ice V to XIII and Ice VI to XV Hydrogen-Ordering Phase Transitions. *J. Chem. Phys.* **2018**, *148* (24). https://doi.org/10.1063/1.5022159.

(9) Salzmann, C. G.; Rosu-Finsen, A.; Sharif, Z.; Radaelli, P. G.; Finney, J. L. Detailed Crystallographic Analysis of the Ice V to Ice XIII Hydrogen-Ordering Phase Transition. *J. Chem. Phys.* **2021**, *154* (13), 134504. https://doi.org/10.1063/5.0045443.

(10) Shephard, J. J.; Salzmann, C. G. The Complex Kinetics of the Ice VI to Ice XV Hydrogen Ordering Phase Transition. *Chem. Phys. Lett.* **2015**, *637*, 63–66. https://doi.org/10.1016/j.cplett.2015.07.064.

(11) Salzmann, C. G.; Slater, B.; Radaelli, P. G.; Finney, J. L.; Shephard, J. J.; Rosillo-Lopez, M.; Hindley, J. Detailed Crystallographic Analysis of the Ice VI to Ice XV Hydrogen Ordering Phase Transition. *J. Chem. Phys.* **2016**, *145* (20). https://doi.org/10.1063/1.4967167.

(12) Salzmann, C. G.; Hallbrucker, A.; Finney, J. L.; Mayer, E. Raman Spectroscopic Features of Hydrogen-Ordering in Ice XII. *Chem. Phys. Lett.* **2006**, *429* (4–6), 469–473. https://doi.org/10.1016/j.cplett.2006.08.079.

(13) Köster, K. W.; Fuentes-Landete, V.; Raidt, A.; Seidl, M.; Gainaru, C.; Loerting, T.; Böhmer, R. Dynamics Enhanced by HCl Doping Triggers 60% Pauling Entropy Release at the Ice XII–XIV Transition. *Nat. Commun.* **2015**, *6* (1), 7349. https://doi.org/10.1038/ncomms8349.

(14) Fuentes-Landete, V.; Köster, K. W.; Böhmer, R.; Loerting, T. Thermodynamic and Kinetic Isotope Effects on the Order–Disorder Transition of Ice XIV to Ice XII. *Phys. Chem. Chem. Phys.* **2018**, *20* (33), 21607–21616. https://doi.org/10.1039/C8CP03786H.

(15) Bridgman, P. W. The Pressure-Volume-Temperature Relations of the Liquid, and the Phase Diagram of Heavy Water. *J. Chem. Phys.* **1935**, *3* (10), 597–605. https://doi.org/10.1063/1.1749561.

(16) Millot, M.; Coppari, F.; Rygg, J. R.; Correa Barrios, A.; Hamel, S.; Swift, D. C.; Eggert, J. H. Nanosecond X-Ray Diffraction of Shock-Compressed Superionic Water Ice. *Nature* **2019**, *569* (7755), 251–255. https://doi.org/10.1038/s41586-019-1114-6.

(17) Shephard, J. J.; Ling, S.; Sosso, G. C.; Michaelides, A.; Slater, B.; Salzmann, C. G. Is High-Density Amorphous Ice Simply a "Derailed" State along the Ice I to Ice IV Pathway? *J. Phys. Chem. Lett.* **2017**, *8* (7), 1645–1650. https://doi.org/10.1021/acs.jpclett.7b00492.

(18) Martelli, F.; Giovambattista, N.; Torquato, S.; Car, R. Searching for Crystal-Ice Domains in Amorphous Ices. *Phys. Rev. Mater.* **2018**, *2* (7), 1–10. https://doi.org/10.1103/PhysRevMaterials.2.075601.

(19) Salzmann, C. G.; Kohl, I.; Loerting, T.; Mayer, E.; Hallbrucker, A. Raman Spectroscopic Study on Hydrogen Bonding in Recovered Ice IV. *J. Phys. Chem. B* **2003**, *107* (12), 2802–2807. https://doi.org/10.1021/jp021534k.

(20) Salzmann, C. G.; Radaelli, P. G.; Slater, B.; Finney, J. L. The Polymorphism of Ice: Five Unresolved Questions. *Phys. Chem. Chem. Phys.* **2011**, *13* (41), 18468. https://doi.org/10.1039/c1cp21712g.

(21) Rosu-Finsen, A.; Salzmann, C. G. Is Pressure the Key to Hydrogen Ordering Ice IV? *Chem. Phys. Lett.* **2022**, *789* (October 2021), 139325. https://doi.org/10.1016/j.cplett.2021.139325.

(22) Hattori, T.; Sano-Furukawa, A.; Arima, H.; Komatsu, K.; Yamada, A.; Inamura, Y.; Nakatani, T.; Seto, Y.; Nagai, T.; Utsumi, W.; Iitaka, T.; Kagi, H.; Katayama, Y.; Inoue, T.; Otomo, T.; Suzuya, K.; Kamiyama, T.; Arai, M.; Yagi, T. Design and Performance of High-Pressure PLANET Beamline at Pulsed Neutron Source at J-PARC. *Nucl. Instruments Methods Phys. Res. Sect. A Accel. Spectrometers, Detect. Assoc. Equip.* **2015**, *780*, 55–67. https://doi.org/10.1016/j.nima.2015.01.059.

(23) Komatsu, K.; Moriyama, M.; Koizumi, T.; Nakayama, K.; Kagi, H.; Abe, J.; Harjo, S. Development of a New P–T Controlling System for Neutron-Scattering Experiments. *High Press. Res.* **2013**, *33* (1), 208–213. https://doi.org/10.1080/08957959.2012.762914.

(24) Salzmann, C. G.; Loerting, T.; Kohl, I.; Mayer, E.; Hallbrucker, A. Pure Ice IV from High-Density Amorphous Ice. *J. Phys. Chem. B* **2002**, *106* (22), 5587–5590. https://doi.org/10.1021/jp014391v.

(25) Engelhardt, H.; Kamb, B. Structure of Ice IV, a Metastable High-Pressure Phase. *J. Chem. Phys.* **1981**, *75* (12), 5887–5899. https://doi.org/10.1063/1.442040.

(26) Komatsu, K.; Noritake, F.; Machida, S.; Sano-Furukawa, A.; Hattori, T.; Yamane, R.; Kagi, H. Partially Ordered State of Ice XV. *Sci. Rep.* **2016**, *6* (1), 28920. https://doi.org/10.1038/srep28920.

(27) Hauschild, E.; Tonauer, C.; Eisendle, S.; Landete, V. F.; Yamashita, K.; Hoffmann, L.; Böhmer, R.; Loerting, T. Highly Ordered Deuterated Ice XIV. *Res. Sq.* **2022**. https://doi.org/10.21203/RS.3.RS-1908887/V1.

(28) Komatsu, K. Neutrons Meet Ice Polymorphs. *Crystallogr. Rev.* **2022**, 1–74. https://doi.org/10.1080/0889311X.2022.2127148.

(29) Strässle, T.; Klotz, S.; Kunc, K.; Pomjakushin, V.; White, J. S. Equation of State of Lead from High-Pressure Neutron Diffraction up to 8.9 GPa and Its Implication for the NaCl Pressure Scale. *Phys. Rev. B - Condens. Matter Mater. Phys.* **2014**, *90* (1), 1–8. https://doi.org/10.1103/PhysRevB.90.014101.

(30) Larson, A. C.; Dreele, R. B. Von. GSAS, General Structure Analysis System. 2000.

(31) Toby, B. H. EXPGUI, a Graphical User Interface for GSAS. *J. Appl. Crystallogr.* **2001**, *34* (2), 210–213. https://doi.org/10.1107/S0021889801002242.

(32) Momma, K.; Izumi, F. VESTA 3 for Three-Dimensional Visualization of Crystal, Volumetric and Morphology Data. *J. Appl. Crystallogr.* **2011**, *44* (6), 1272–1276. https://doi.org/10.1107/S0021889811038970.